Effects of thermo-osmosis on hydraulic behaviour of saturated clays

Renato Zagorščak[1], Majid Sedighi[2, 3] and Hywel R. Thomas[4]

[1] Ph.D. Student, Geoenvironmental Research Centre, School of Engineering, Cardiff University, The Queen's Buildings, The Parade, Cardiff, CF24 3AA, United Kingdom (corresponding author). E-mail: ZagorscakR@cardiff.ac.uk

[2] Research Fellow, Geoenvironmental Research Centre, School of Engineering, Cardiff University, The Queen's Buildings, The Parade, Cardiff, CF24 3AA, United Kingdom.

[3] Lecturer, School of Mechanical, Aerospace and Civil Engineering, The University of Manchester, Sackville Street, Manchester, M1 9PL, United Kingdom (current affiliation). E-mail: majid.sedighi@manchester.ac.uk

[4] Professor, Geoenvironmental Research Centre, School of Engineering, Cardiff University, The Queen's Buildings, The Parade, Cardiff, CF24 3AA, United Kingdom. E-mail: ThomasHR@cardiff.ac.uk

Abstract

Despite a body of research carried out on thermally coupled processes in soils, understanding of thermo-osmosis phenomena in clays and its effects on hydro-mechanical behaviour is incomplete. This paper presents an investigation on the effects of thermo-osmosis on hydraulic behaviour of saturated clays. A theoretical formulation for hydraulic behaviour is developed incorporating an explicit description of thermo-osmosis effects on coupled hydro-mechanical behaviour. The extended formulation is implemented within a coupled numerical model for thermal, hydraulic, chemical and mechanical behaviour of soils. The model is tested and applied to simulate a soil heating experiment. It is shown that the inclusion of thermo-osmosis in the coupled thermo-hydraulic simulation of the case study provides a

better agreement with the experimental data compared with the case where only thermal expansion of the soil constituents was considered. A series of numerical simulations are also presented studying the pore water pressure development in saturated clay induced by a heating source. It is shown that pore water pressure evolution can be considerably affected by thermo-osmosis. Under the conditions of the problem considered, it was found that thermo-osmosis changed the pore water pressure regime in the vicinity of the heater in the case where value of thermo-osmotic conductivity was larger than 10^{-12} $m^2.K^{-1}.s^{-1}$. New insights into the hydraulic response of the ground and the pore pressure evolution due to thermo-osmosis are provided in this paper.

Keywords

Thermo-osmosis; saturated clay; hydraulic behaviour; coupled modelling; hydro-mechanical

Introduction

Temperature variations can induce various processes and changes in soil-water system and affect the engineering behaviour of soil. In many engineering applications, considerable changes in ground temperature can be expected. Examples are i) the geological disposal of high level radioactive waste where elevated temperature is generated by the waste and ii) ground source heat or energy foundations where thermal gradients in the soil are induced by exchanging heat with the ground. Understanding the processes and parameters involved in the behaviour of soils under non-isothermal conditions is therefore of importance for performance analysis and sustainable design of various geo-structures.

It has been previously shown that heating of soils can cause pore water pressure development and contraction/dilation in the soil depending on the stress history (Campanella and Mitchell 1968; Towhata et al. 1993; Sultan et al. 2002; Laloui and François 2009). Observations from a field experiment of heat storage in clay have indicated that by applying a temperature gradient, an excess pore water pressure has developed during the heating period which has resulted in a considerable settlement after pore water pressure dissipation (Moritz and Gabrielsson 2001). The difference between the thermal expansion properties of water and solid particles of soil has been described as being the most influential mechanism for pore water pressure development in saturated soils (Mitchell 1993).

Osmosis phenomena are among key processes controlling the water flow, chemical transport and deformation behaviour of clays. Under non-isothermal conditions, thermo-osmosis is a coupled mechanism that describes fluid flow in saturated clays under a temperature gradient. From a thermodynamics point of view, thermo-osmosis is controlled by the enthalpy difference between the free water/fluid in the clay pores and the pore water affected by the

65 clay interactions (Gonçalvès and Trémosa 2010). In particular, the presence of an electric
66 field normal to the clay mineral surface modifies the structure and properties of the fluid at
67 the solid surface which causes an alteration of the specific enthalpy of the solution in the pore
68 space. Due to such alteration, a positive change in enthalpy can cause a liquid flow from the
69 warm to the cold side of a sample (Gonçalvès and Trémosa 2010). Despite a significant body
70 of research studying the hydraulic behaviour of saturated and unsaturated clays, limited
71 studies have discussed the effects of thermo-osmosis on the overall thermo-hydro-mechanical
72 behaviour of saturated soils.

73 The soil property associated with thermo-osmosis is expressed by the thermo-osmotic
74 conductivity which has been reported to be in the range of 10^{-14}-10^{-10} $m^2.K^{-1}.s^{-1}$ (Dirksen
75 1969; Soler 2001; Zheng and Samper 2008; Ghassemi et al. 2009). Due to the wide range of
76 values reported in the literature, the impact of thermo-osmotic conductivity value on pore
77 water pressure evolution and fluid flow near a heat source is still unclear. While it can be
78 expected that the effect of thermo-osmosis on pore water pressure evolution becomes more
79 significant with an increase in the magnitude and duration of a heat emission due to the
80 established thermal gradient in the vicinity of the heat source, further understanding on the
81 importance of thermo-osmosis on such behaviour is required.

82 Experimental investigations have demonstrated the effects of thermo-osmosis on water flow
83 under temperature gradient in saturated clays (e.g. Dirksen 1969; Trémosa et al. 2010).
84 Dirksen (1969) has reported the flow of water in compacted saturated clays induced by
85 applying a temperature gradient. Trémosa et al. (2010) have reported a series of in-situ
86 experiments where the importance of thermo-osmosis on water flow in clay-rock has been
87 examined. The results have suggested that thermo-osmosis can affect the water flow and
88 contribute to the excess pore pressure observations in impervious rocks. Gonçalvès et al.

89 (2012) have reported that in low porosity saturated clays, the water flow induced by a
90 temperature gradient occurs from the warm boundary to the cold boundary whilst in high-
91 porosity soils with a weak thermo-osmotic property, the water flow can occur in the opposite
92 direction of the temperature gradient.

93 Recent studies have indicated that the electro-chemical interactions in the water-clay
94 interface correlate with thermo-osmotic properties (Gonçalvès and Trémosa 2010; Gonçalvès
95 et al. 2012). An expression for the thermo-osmotic conductivity considering the enthalpy
96 change due to hydrogen bonding to the clay surfaces has been suggested by Gonçalvès et al.
97 (2012). Correlations have been provided between thermo-osmotic permeability and intrinsic
98 permeability for different clays which indicate that the ratio of thermo-osmotic conductivity
99 to the intrinsic permeability is strongly correlated with the electrochemical properties of the
100 soil (Gonçalvès et al. 2012). For most of the soils, the ratio falls within a range of $10\text{-}10^3$
101 $Pa.K^{-1}$, while for some shales it can be up to 10^8 $Pa.K^{-1}$ (Gonçalvès et al. 2012).

102 A limited number of modelling studies exist describing the effects of thermo-osmosis on
103 coupled thermo-hydraulic and thermo-hydro-mechanical behaviour of saturated clays. A
104 coupled thermo-poroelastic numerical investigation on semi-impermeable clay barriers has
105 been presented by Zhou et al. (1998) which considers compressibility, thermal expansion of
106 constituents and thermo-osmosis. Sánchez et al. (2010) have studied the thermo-hydro-
107 mechanical behaviour based on the results of a mock-up heating test with a special emphasis
108 on the effect of the thermo-osmotic flow in the hydration of the clay barrier. The results of
109 this study have indicated that the inclusion of the thermo-osmotic flow in the analysis of
110 moisture migration has improved the accuracy of the model prediction. Zheng et al. (2011)
111 have presented a numerical investigation of the coupled thermal, hydraulic and chemical
112 behaviour of compacted clay including the effects of thermo-osmosis. The results of

sensitivity analyses presented by Zheng et al. (2011) have indicated that the water contents and dissolved concentrations are strongly sensitive to the intrinsic permeability and the thermo-osmotic permeability. Furthermore, authors have concluded that chemical osmosis is of less importance comparing to Darcian flux and thermo-osmosis. An analysis of the pore pressure distribution in shale formations under thermal, hydraulic, chemical and electrical interactions has been conducted by Roshan and Aghighi (2012). Authors have shown that thermo-osmosis plays a considerable effect on the pore pressure evolution when considering the temperature gradient between the formation and the drilling fluid. Chen et al. (2013) have studied the effect of positive and negative thermo-osmotic coefficients on pore water pressure evolution in low porous material. A conclusion has been made that thermo-osmosis can have a strong influence on water transport and mechanical deformation. Further research needs have been suggested as a result of this work to obtain a better understanding of the direction of the water flow in the domain.

More recently, Yang et al. (2014) have presented an analytical model for the coupled effect of thermo-osmosis in saturated porous medium and studied the pore pressure and stress variations of clay under thermal effects. Similarly, Roshan et al. (2015) have developed an analytical solution for a thermo-osmotic test that includes the effects of the solid-thermal expansion and thermo-osmosis. By conducting a series of thermo-osmotic experiments and further analysis using the analytical model, authors have concluded that for the correct interpretation of experimental data, it is important that both solid-fluid thermal expansion and thermo-osmosis are considered in the analysis.

This paper presents the development of a formulation and a numerical model for coupled thermal, hydraulic and mechanical behaviour of saturated clay with emphasis on studying the effects of thermo-osmosis on hydraulic behaviour. A formulation of water flow is presented

which is implemented within an existing numerical model of coupled thermal, hydraulic, chemical and mechanical behaviour of unsaturated soils (Thomas and He 1997; Thomas et al. 2003; Sedighi et al. 2016). The results of a series of numerical investigations are presented to test the implementation of the formulation in the model. The effects of thermo-osmosis are considered by comparison with analytical and experimental benchmarks. In addition, a series of numerical simulations are presented which aim to investigate the effects of thermo-osmosis on pore water pressure development around a heat source.

Theoretical formulation and numerical model

The formulation presented below is based on the general formulation of coupled thermal, hydraulic and mechanical behaviour (THM) for unsaturated soils presented by Thomas and He (1997). A simplified form of the coupled THM formulation for saturated clays is extended here which considers the effects of thermo-osmosis in hydraulic behaviour. It is noted that the focus of the paper is on the effects of thermo-osmosis on hydraulic behaviour; hence a simplified mechanical formulation is adopted and included in the governing equations for water flow. The system is fully saturated; therefore the vapour flow is not considered.

Hydraulic behaviour

The governing equation of water flow is considered based on the principle of mass conservation and following the formulation provided by Thomas and He (1997). This can be expressed as (Thomas and He 1997):

$$\frac{\partial}{\partial t}(\rho_l \theta_l \delta V) = -\delta V \nabla \cdot (\rho_l v_l) \tag{1}$$

where t is time, ρ_l is the density of liquid water, θ_l is the volumetric water content, ∇ is the gradient operator and δV is the incremental volume of the soil. v_l is the velocity of liquid that is calculated based on Darcy's law for water flow in saturated soils.

Expanding equation (1) for fully saturated clay with respect to its partial derivatives and using an incremental volume as a summation of the void volume and solid volume yields:

$$e\delta V_s \frac{\partial \rho_l}{\partial t} + \rho_l \delta V_s \frac{\partial e}{\partial t} + \rho_l e \frac{\partial (\delta V_s)}{\partial t} = -\delta V_s (1+e) \nabla \cdot (\rho_l v_l) \tag{2}$$

where δV_s is the increment volume of the solids and e stands for the void ratio of soil.

Dividing equation (2) by δV_s and $(1+e)$, yields:

$$n \frac{\partial \rho_l}{\partial t} + \rho_l \frac{\partial e}{\partial t(1+e)} + \rho_l n \frac{1}{\delta V_s} \frac{\partial (\delta V_s)}{\partial t} = -\nabla \cdot (\rho_l v_l) \tag{3}$$

For a deformable soil the term $\partial e / \partial t(1+e)$ can be expressed as $\partial \varepsilon_v / \partial t$, where ε_v is the volumetric strain that is, by definition, the rate of change of the void ratio with respect to the initial volume. The total volumetric elastic strain should include the contributions of thermal expansion and effective stress which can be presented as (Thomas and He 1997; Hueckel et al. 2011); therefore:

$$\frac{\partial \varepsilon_v}{\partial t} = \alpha \frac{\partial T}{\partial t} - m_v \frac{\partial \sigma'}{\partial t} \tag{4}$$

where α is the thermal expansion coefficient of the soil structure, m_v is the coefficient of soil compressibility, T is the temperature and σ' is the effective stress which is based on Terzaghi's effective stress principle equal to $\sigma' = \sigma - u_l$ where σ is the total stress and u_l is the pore water pressure. Thermal expansion coefficient of the soil structure is a negative value if an increase in temperature causes a decrease in volume (Mitchell 1993; Thomas et al. 1996).

175 Assuming a constant mass of the solid phase, the temporal variation of the solid volume is
176 equal to the temporal variation of the solid density, given as:

$$\frac{1}{\delta V_s}\frac{\partial(\delta V_s)}{\partial t} = -\frac{1}{\rho_s}\frac{\partial(\rho_s)}{\partial t} \tag{5}$$

177 where ρ_s is density of the solid phase.

178 The density of liquid phase can be presented as a function of water pressure and temperature
179 (François et al. 2009); therefore:

$$\frac{\partial(\rho_l)}{\partial t} = \rho_l\beta_l\frac{\partial u_l}{\partial t} - \rho_l\beta_l'\frac{\partial T}{\partial t} \tag{6}$$

180 where β_l is the compressibility coefficient of liquid water and β_l' is the thermal expansion
181 coefficient of water.

182 The solid grains are assumed to be incompressible by stress. Therefore the density of the
183 solid phase is expressed only as a function of temperature:

$$\frac{\partial(\rho_s)}{\partial t} = -\rho_s\beta_s'\frac{\partial T}{\partial t} \tag{7}$$

184 where β_s' is the thermal expansion coefficient of solid particles.

185 Replacing equations (4) to (7) into equation (3) and rearranging the similar terms, yields:

$$\rho_l[n\beta_l + m_v]\frac{\partial u_l}{\partial t} + \rho_l[n(\beta_s' - \beta_l') + \alpha]\frac{\partial T}{\partial t} - \rho_l m_v\frac{\partial \sigma}{\partial t} = -\nabla\cdot(\rho_l\mathbf{v}_l) \tag{8}$$

186 The mechanisms of water flow are considered to be due hydraulic, thermo-osmosis and
187 gravitational potentials (Gonçalvès and Trémosa 2010). It is noted that the chemical osmosis
188 is not considered here. Using Darcy's law and considering the potentials for water flow
189 described above, the velocity of liquid can be presented as (Gonçalvès and Trémosa 2010):

$$\mathbf{v}_l = -k_l\left(\frac{\nabla u_l}{\rho_l g} + \frac{k_T}{k_l}\nabla T + \nabla z\right) \tag{9}$$

where k_l is the saturated hydraulic conductivity, k_T stands for the thermo-osmotic conductivity, z is the elevation and g is the gravitational constant.

The general form of water flow described in equation (8) can be extended considering the water flow mechanisms presented in equation (9) as:

$$\rho_l[n\beta_l + m_v]\frac{\partial u_l}{\partial t} + \rho_l[n(\beta_s' - \beta_l') + \alpha]\frac{\partial T}{\partial t} - \rho_l m_v \frac{\partial \sigma}{\partial t} = \nabla \cdot \left(\frac{k_l}{g}\nabla u_l\right) + \nabla \cdot (k_T \rho_l \nabla T) + \nabla \cdot (k_l \rho_l \nabla z) \quad (10)$$

Equation (10) can be further simplified under the constant total stress as:

$$\rho_l[n\beta_l + m_v]\frac{\partial u_l}{\partial t} + \rho_l[n(\beta_s' - \beta_l') + \alpha]\frac{\partial T}{\partial t} = \nabla \cdot \left(\frac{k_l}{g}\nabla u_l\right) + \nabla \cdot (k_T \rho_l \nabla T) + \nabla \cdot (k_l \rho_l \nabla z) \quad (11)$$

Thermal behaviour

The governing equation of heat transfer has been developed based on the energy conservation law in unsaturated porous media (Thomas and He 1997). Based on the formulation presented in Thomas and He (1997), the governing equation of heat transfer in saturated soil can be presented as:

$$\frac{\partial}{\partial t}[H_c(T - T_r)] = -\delta V \nabla \cdot [-\lambda_T \nabla T + A(T - T_r)] \quad (12)$$

where H_c is the heat storage capacity, T_r represents the reference temperature, λ_T is the thermal conductivity and A stands for the sum of the heat convection components.

Details of the expanded formulation for the governing equations of heat transfer presented in equation (12) can be found in Thomas and He (1997).

Numerical model development

205 The formulation of water flow is implemented within an existing numerical model
206 (COMPASS) developed at the Geoenvironmental Research Centre, Cardiff University which
207 is based on finite element and finite difference methods (Thomas and He 1997; Thomas et al.
208 2012). The Galerkine weighted residual method has been adopted by which the spatial
209 discretisation is developed and the temporal discretisation is achieved by applying an implicit
210 finite difference algorithm (Thomas and He 1997; Seetharam et al. 2011; Sedighi et al. 2016).
211 The model has been extensively tested, applied and extended to study the coupled behaviour
212 of unsaturated soils, in particular, the behaviour of highly compacted swelling clays in
213 relation to geological disposal of high level radioactive waste (e.g. Thomas et al. 2003; Cleall
214 et al. 2007; Vardon et al. 2011; Thomas and Sedighi 2012). The chemistry of clay-water
215 interaction and the effects on coupled processes of highly compacted swelling clays have
216 recently been integrated in the model (Sedighi 2011; Sedighi and Thomas 2014). Details of
217 the numerical formulation and computational aspects have been discussed in previous
218 publications; therefore the details are not repeated here.

219 The components of the hydraulic behaviour considering thermo-osmosis, thermal expansion
220 relationships and associated parameters of consolidation presented in equation (11) are
221 implemented in the numerical model. It is noted that the application of the model presented in
222 this paper is under constant total stress. Therefore the simulations have been carried using the
223 thermo-hydraulic modules of the model.

224

225 Verification under steady state conditions

226 Inclusion of the thermo-osmosis formulation in the water flow equation (equation 11) in the
227 numerical model is tested here. The problem considered is a fully saturated clay where a

fixed temperature gradient in the system causes a gradient of water pressure. As the flow occurs horizontally, the gravitational effects can be neglected. Under these conditions, the temporal variations of temperature and pore water pressure become zero and equation (11) can be simplified as:

$$\frac{k_l}{g}\nabla u_l = -k_T \rho_l \nabla T \tag{13}$$

This section presents the results of a verification test on the inclusion of thermo-osmosis component for moisture flow in comparison with the above algebraic equation and under the same conditions. A two dimensional soil domain (1.0 × 0.1 m) is considered in this simulation. The soil is assumed to be fully saturated. Temperatures at the boundaries are assumed to be fixed values, i.e. 300K and 285K which provide a constant temperature gradient over the domain at steady-state condition. The water pressure is considered fixed at the boundary with lower temperature while the other side of the domain is considered as an impermeable boundary for water flow. The initial pore water pressure is assumed to be equal to the water pressure at the boundary, i.e. 100 kPa.

The domain is discretised into 100 equally sized 4-nodded quadrilateral elements. A constant time-step of 3600 seconds is considered. Material parameters used in the simulation are presented in Table 1.

By knowing the temperature gradient in the system, the gradient of water pressure can be analytically calculated at steady state using equation (13). For the conditions and parameters used in this problem, the gradient of pore water pressure can be given as:

$$\nabla u_l = -\frac{5.0 \times 10^{-12} \times 998.0 \times 9.81}{1.0 \times 10^{-11}} \times \frac{285 - 300}{1} = 73427.85 \text{ Pa. m}^{-1}$$

247 The pore water pressure at the left hand side boundary with temperature of 300K is therefore
248 obtained to be qual to 26572.15 Pa.

249 Fig. 1 presents the profile of water presurre in the domain. The same value for the gradient of
250 pore water pressure is obtained from the numerical results as that calculated from the
251 analytical solution. It can be observed that the pore pressure decreases in the warmer
252 boundary of the domain due to the thermo-osmosis effect in order to maintain the overall
253 water potential balance in the system.

254

255 Pore water pressure development in a heating experiment

256 In order to examine the effects of thermo-osmosis in pore water pressure development under
257 non-isothermal conditions, numerical simulations are carried out based on a field scale
258 heating experiment (ATLAS test) carried out in Mol, Belgium in an underground research
259 facility at a depth of 223 m in Boom Clay (François et al. 2009; Chen et al. 2011). The
260 simulation conditions including the domain, initial conditions and boundary conditions are
261 selected based on the experimental conditions described in François et al. (2009). The
262 numerical analysis includes studying the pore water pressure generation due to thermal load
263 through two series of analysis: i) without considering thermo-osmosis in the analysis and ii)
264 by including the thermo-osmosis effects.

265 The simulation problem is a 100 m axisymmetric domain where the inner boundary is
266 impermeable for flow. At the inner boundary, temperature is instantaneously increased by
267 45K from the initial value of 289.5K and kept constant for 3 years. Temperature is then
268 increased by 40K and kept constant for 11 months after which it is restored back to the initial
269 temperature and remains constant until the end of the simulation. At the outer boundary, the

temperature and the pore water pressure are fixed at the same value of the initial condition, i.e. 289.5K and 2.025 MPa, respectively.

The physical properties of Boom Clay have been presented in several published works (e.g. Baldi et al. 1988; Hong et al. 2013; Hueckel and Baldi 1990; Sultan et al. 2002; Cui et al. 2009; François et al. 2009; Chen et al. 2011). A summary of the material properties used in this study is presented in Table 2. For the sake of simplicity, the outlined parameters are taken as constants in the numerical simulation. The value of thermo-osmotic permeability is calculated based on data presented in Gonçalvès and Trémosa (2010) and Gonçalvès et al. (2012) who provided a ratio of osmotic permeability to intrinsic permeability (k), i.e. k_T/k as a function of half-pore thickness of the porous media. Using the specific surface area values ranging between 150 $m^2.g^{-1}$ and 163 $m^2.g^{-1}$ presented in Deng et al. (2011) and half-pore thickness equation in Gonçalvès et al. (2012), a value for half-pore thickness of approximately 1.5nm for the Boom clay is calculated. Hence, following Gonçalvès and Trémosa (2010) and Gonçalvès et al. (2012), an approximate value for thermo-osmotic conductivity of 3×10^{-12} $m^2.K^{-1}.s^{-1}$ is chosen. It is noted that in the absence of exact values for thermo-osmotic conductivity, the approximated value may involve a level of uncertainty, yet providing a reasonable value to be used for investigating the effect of thermo-osmosis phenomenon on pore water pressure development in this example.

The domain is discretised to 300 unequally sized 4-nodded quadrilateral elements. A maximum time-step of one week is considered for the simulations for a total period of 2,500 days.

Fig. 2 presents the results of temperature variation with time at 1.183 m distance from the symmetrical axis of the domain. The results are compared with those observed in the

293 experiment (François et al. 2009). From Fig. 2, it can be observed that the modelling results
294 are in close agreement with the experimental data. The numerical results show a slight
295 overestimation of the temperature evolution during the stages of temperature increase, while
296 the numerical results agree well with the experimental data at the stages where temperature
297 has been restored back to the initial soil temperature.

298 The results of the pore water pressure development with time at 1.183 m distance from
299 symmetrical axis are presented in Fig. 3. Experimental data are also shown in Fig. 3. Two
300 series of results from the numerical analysis are presented including the results of modelling
301 without thermo-osmosis effects and those with this effect. The pore water pressure
302 development in the analysis without thermo-osmosis is only related to thermal expansion
303 effect. The numerical trend obtained is similar to the observation in the experiment. However,
304 there are considerable discrepancies in terms of pore water dissipation at the end of both
305 heating phases when temperature stabilised. In other words, the simulation without thermo-
306 osmosis effect over-predicts the pore water pressure development. It can be observed that
307 closer agreements with the experimental data are achieved when combined effects of thermo-
308 osmosis and thermal expansion are considered in the simulations. The phenomenon can be
309 explained by analysing the effect of thermo-osmosis on the fluid flow. Water flow is
310 diverging from the warmer side towards the colder side of the domain causing a pressure
311 decrease closer to the heat source. From the results presented in Fig. 3, it can be observed that
312 during the stage at which temperature is stable, the thermo-osmosis contributes to the pore
313 water pressure decrease. A similar observation has been presented in the work of Trémosa et
314 al. (2010) where after an applied temperature pulse, the contribution of thermo-osmosis to the
315 pore water pressure dissipation was found to be more pronounced than the reduction of the
316 water volume due to the temperature decrease.

317 The results of the numerical model show good agreement with the first pore water dissipation
318 stage while the results for the second and the third dissipation stages show slightly different
319 pressure values compared with the experimental data. However, the general trend
320 demonstrates a similar qualitative trend observed in the experiment. The discrepancies
321 observed both for temperature and pore pressure evolutions may be related to various factors
322 including the heat diffusion and liquid flow via radial direction (axisymmetric analysis), the
323 approximated value for thermo-osmotic conductivity, duration of the simulation and constant
324 values considered for the parameters used in the numerical simulation.

325

326 ## Simulation of thermo-osmosis effects

327 ### Numerical analysis

328 This section provides the results of a series of numerical simulations on the hydraulic
329 behaviour of clay around a heating source. The aim of the simulations is to investigate the
330 effects of thermo-osmosis on temporal and spatial pore water pressure developments around a
331 heating source in saturated clay.

332 The problem studied is a two dimensional saturated soil domain (30 m × 1 m) which is heated
333 at one boundary by a heating source 0.6 m in diameter. An axisymmetric analysis is
334 considered where the axis of the symmetry is at the centre of the heat source. The internal
335 boundary of the model corresponds to the external boundary of the heat source, which is 0.3
336 m away from the axis of the symmetry. The external boundary of the model is placed at 30.3
337 m from the symmetrical axis of the domain. The inner boundary condition is considered as an
338 impermeable and adiabatic where a time curve is applied for temperature values.
339 Temperature is constantly increasing from an initial value of 285K for the first 2 days until it

reaches a fixed value at 310K and then remains constant throughout the rest of the computation. At the external boundary, temperature and the pore water pressure are fixed to be the same as the initial condition values of 285K and 100 kPa, respectively.

The domain is discretised to 300 equally sized 4-noded quadrilateral elements. A maximum time-step of 2 hours (7200 seconds) is considered and the duration of the simulation is 30 days.

The soil parameters used in the simulations are summarised in Table 3. The simulation is carried out using three values of thermo-osmotic conductivity based on the range of (k_T/k) provided by Gonçalvès et al. (2012) given as $k_T/k = 10$, $k_T/k = 100$ and $k_T/k = 1000$. The variation of water viscosity with temperature is not considered following the approach presented in Soler (2001) and Ghassemi and Diek (2002) and a constant value of 10^{-3} Pa.s at 20 °C is selected.

It should be noted that the thermo-osmotic conductivity is calculated with respect to intrinsic permeability with a value of 3.3×10^{-17} m^2. As described by Goncalves et al. (2012), this ratio is expressed in $Pa.K^{-1}$ which means that the intrinsic permeability has to be divided by the viscosity first in order to obtain the value of k_T in $m^2.K^{-1}.s^{-1}$. Therefore, water viscosity is taken as a constant value at 20^oC.

The compressibility of the studied soils is calculated based on the specific surface area yielding an approximate value of coefficient of soil volume compressibility. A reference value of the specific surface area of 30 $m^2.g^{-1}$ is taken (Goncalves et al. 2012). Using approach proposed in Mitchell (1993) where an empirical relation between liquid limit and specific surface is given, a liquid limit is obtained through which an approximate value of coefficient of consolidation is assumed. Hence, using the obtained value for coefficient of

363 consolidation and known value of hydraulic conductivity, an approximate value of coefficient
364 of soil volume compressibility of 3.3×10^{-8} Pa^{-1} is calculated and used in the simulation which
365 falls within a range of compressibility values for medium-hard clays.

366 The results of simulations using different coefficients of thermo-osmotic conductivity are
367 presented and compared with the case where only thermal expansion is considered. Fig. 4
368 presents the variation of pore water pressure with time at the heat source and soil interface
369 boundary. It can be observed that for the lowest value of thermo-osmotic conductivity used,
370 i.e. 3.4×10^{-13} $m^2.K^{-1}.s^{-1}$, the difference between the pore water pressure development in
371 comparison with the case where only thermal expansion was considered is negligible, while
372 for the higher values of thermo-osmotic conductivity the difference is more highlighted. As it
373 can be observed after 5 days of heating, the pore water pressure value at the interface is
374 14.1% less when $k_T = 3.4\times10^{-11}$ $m^2.K^{-1}.s^{-1}$ is used, compared to the analysis without thermo-
375 osmosis contribution.

376 Due to the liquid flow caused by the temperature gradient in the domain, it can be expected
377 that the rate of pressure drop would only enhance with time. This can be confirmed from Fig.
378 4 where after 25 days, pressure drop caused by thermo-osmosis increases to 16.31% for the
379 case of $k_T = 3.4\times10^{-11}$ $m^2.K^{-1}.s^{-1}$ in comparison with the results of simulations with thermal
380 expansion only.

381 Temperature profiles in the domain after 2, 7 and 30 days are presented in Fig. 5. After 30
382 days of heating at a constant temperature of 310 K, heat propagates up to a distance of
383 approximately 3.5 m from the heat source creating a temperature gradient in the domain.

384 Further discussion on the spatial variation of pore pressure development in the domain is
385 presented for the simulation with high thermo-osmotic conductivity of 3.4×10^{-11} $m^2.K^{-1}.s^{-1}$. In

386 addition, the results are compared with the case where only thermal expansion is included in
387 the simulation. Profiles of the pore water pressure in the domain for the case of the thermo-
388 osmotic conductivity of 3.4×10^{-11} $m^2.K^{-1}.s^{-1}$ are shown in Fig. 6. The results are presented for
389 three different heating periods, i.e. 2 days, 7 days and 30 days after the start of the simulation.

390 The difference in pore water pressure evolution between the cases without and with the effect
391 of thermo-osmosis is considerable as shown in Fig 6. It can be observed that after 2 days of
392 heating, thermo-osmosis affects the pore water pressure evolution next to the heat source
393 yielding a reduction in the pore water pressure value for 12% in comparison to the case with
394 thermal expansion only. Due to the temperature gradient established in the vicinity of a heat
395 source, the effect of thermo-osmosis becomes more pronounced with an increase in
396 simulation time yielding a reduction in pore water pressure of 15% and 17% after 7 and 30
397 days, respectively. In addition, it can be seen that the pore water pressure almost returns to
398 the initial value at the interface after 30 days of heating due to thermo-osmosis effect. As a
399 consequence of water flowing away from the heat source under the temperature gradient, the
400 water pressure is slowly increasing further away in the domain.

401 **The effects of thermo-osmosis**

402 The results demonstrate the relative importance of thermally driven flow on pore water
403 pressure in the case of high thermo-osmotic properties. Under the conditions of the
404 simulations presented, it can be concluded that values of thermo-osmotic conductivity larger
405 than 10^{-12} $m^2.K^{-1}.s^{-1}$ can affect the water pressure field around the heat source. This
406 conclusion is in agreement with the observation reported in Soler (2001) who has performed
407 simple one-dimensional transport simulations including thermal and chemical osmosis,
408 hyper-filtration and thermal diffusion with the objective of estimating the effects of different

409 coupled transport phenomena where a temperature gradient of 0.25 $K.m^{-1}$ has been used.
410 Author has concluded that thermo-osmosis will have a significant effect if the value of
411 thermo-osmotic conductivity is larger than 10^{-12} $m^2.K^{-1}.s^{-1}$.

412 As previously mentioned, values of the ratio of thermo-osmotic conductivity and intrinsic
413 permeability against the total ionic content used in this paper are adopted from the data
414 presented by Gonçalvès and Trémosa (2010) and Gonçalvès et al. (2012). This approach
415 adopted provides relationships between the thermo-osmotic conductivity and clay surface-
416 charge, bulk fluid concentration, type of counter ion in the pore water and pore size. In
417 addition, authors have verified it with the available data which ones again confirm the
418 electrochemical control of thermo-osmosis. Hence, for a constant value of intrinsic
419 permeability, coefficient of thermo-osmotic conductivity could be influenced and modified
420 by a combination of the aforementioned soil properties.

421 It is noted that the boundary conditions can have considerable influence on the pore water
422 pressure evolution. In the case study presented, the outer boundary was considered to be a
423 constant pore water pressure representing the far field condition. Under other scenarios where
424 the outer boundary is impermeable or several heat sources are located close to each other, the
425 thermo-osmosis could enhance the pore water pressure and induce local reduction in the
426 effective stress. This could be an important aspect as the reduction in the effective stress
427 could cause deformation and geomechanical instability.

428 Due to the fact that the temperature gradient is the driving potential for thermo-osmosis, the
429 observed phenomenon could be further highlighted in media with low thermal conductivity
430 where a large temperature gradient can develop next to the heat source. Using a value of
431 3.4×10^{-10} $m.s^{-1}$ for hydraulic conductivity in this study, it was observed that water flow both

under pressure gradients and temperature gradients contributes to the overall flow of water in the system. However, in saturated porous media with hydraulic conductivity lower than the abovementioned, liquid flow due to thermo-osmosis could become a dominant process prevailing over a classical Darcian flow. This could be important in the context of a nuclear waste disposal and radionuclide release where high temperature gradient is established in the vicinity of waste packages and thermo-osmosis might contribute to the overall convective transport of water and radionuclides. As this simulation for 30 days of heat emission shows that thermo-osmosis affects the pore water pressure field around the heat source only when relatively high value of thermo-osmotic conductivity is considered, this might not be the case where heat emission lasts for prolonged time periods, i.e. thousands of years for the case of nuclear waste. In such case, it can be expected that even lower values of thermo-osmotic conductivity might contribute to the water flow in low permeability porous media. For such purpose, further research should be undertaken for reliable estimation of the thermo-osmotic conductivity value and its dependence on temperature and soil properties.

Conclusions

The work presented describes the effects of thermo-osmosis phenomenon on hydraulic behaviour of fully saturated soils. The theoretical formulation accommodates thermo-osmosis in the formulation of water flow under coupled thermal, hydraulic and mechanical behaviour. The developed model was tested against an analytical benchmark and a heating experiment in order to examine the accuracy of the model development and implementation. It was shown that the inclusion of thermo-osmosis in the coupled thermo-hydraulic simulation of a heating

454 experiment provides a better agreement with the experimental data compared with the case
455 where only thermal expansion of the soil constituents was considered.

456 A series of simulations were performed that examine the pore water pressure behaviour under
457 heating. Through the numerical simulations presented, it was shown that the thermally driven
458 liquid water flow due to thermo-osmosis can affect the pore water pressure evolution in the
459 vicinity of the heat source. Under the conditions of the simulation related to the clay
460 behaviour subjected to a constant heating source, it was found that the effect of thermo-
461 osmosis is considerable at thermo-osmotic conductivity values larger than 10^{-12} $m^2.K^{-1}.s^{-1}$.

462

463 ## Acknowledgments

464 The work described in this paper has been carried out as a part of the GRC's
465 (Geoenvironmental Research Centre) Seren project, which is funded by the Welsh European
466 Funding Office (WEFO). The financial support is gratefully acknowledged.

467

468 ## References

469 Baldi, G., Hueckel, T. and Pellegrini, R. (1988). "Thermal volume changes of the mineral-
470 water system in low-porosity clay soils." *Canadian Geotechnical Journal*, 25, 807-825.

471 Campanella, R. G. and Mitchell, J. K. (1968). "Influence of temperature variations on soil
472 behavior." *Journal of Geotechnical Engineering ASCE*, 94 (3), 709–734

473 Chen, G. J., Sillen, X., Verstricht, J. and Li, X. L. (2011). "ATLAS III in situ heating test in
474 boom clay: Field data, observation and interpretation." *Computers and Geotechnics*, 38, 683-
475 696.

476 Chen, X. H., Pao, W. and Li, X. (2013). "Coupled thermo-hydro-mechanical model with
477 consideration of thermal-osmosis based on modified mixture theory." *International Journal*
478 *of Engineering Science*, 64, 1-13.

479 Cleall, P. J., Seetharam, S. and Thomas, H. R. (2007). "Inclusion of Some Aspects of
480 Chemical Behavior of Unsaturated Soil in Thermo/Hydro/Chemical/Mechanical Models. I:
481 Model Development." *Journal of Engineering Mechanics,* 10.1061/(ASCE)0733-
482 9399(2007)133:3(338), 338-347.

483 Cui, Y. J., Le, T. T., Tang, A. M., Delage, P. and Li, X. L. (2009). "Investigating the time-
484 dependent behaviour of Boom clay under thermo-mechanical loading." *Géotechnique*, 59:4,
485 319-329.

486 Deng, Y. F., Tang, A. M., Cui, Y. J. and Li, X. L. (2011). "Study on the hydraulic
487 conductivity of Boom clay." *Canadian Geotechnical Journal*, 48, 1461-1470.

488 Dirksen, C. (1969). "Thermo-osmosis through compacted saturated clay membranes." *Soil*
489 *Science Society of America Journal*, 33, 821-826.

490 François, B., Laloui, L. and Laurent, C. (2009). "Thermo-hydro-mechanical simulation of
491 ATLAS in situ large scale test in Boom Clay." *Computers and Geotechnics*, 36, 626-640.

492 Ghassemi, A. and Diek, A. (2002). "Porothermoelasticity for swelling shales." *Journal of*
493 *Petroleum Science and Engineering*, 34 (1-4), 123-135.

494 Ghassemi, A., Tao, Q. and Diek, A. (2009). "Influence of coupled chemo-poro-thermoelastic
495 processes on pore pressure and stress distributions around a wellbore in swelling shale."
496 *Journal of Petroleum Science and Engineering*, 67, 57-64.

497 Gonçalvès, J. and Trémosa, J. (2010). "Estimating thermo-osmotic coefficients in clay-rocks:
498 I. Theoretical insights." *Journal of Colloid and Interface Science*, 342, 166-174.

499 Gonçalvès, J., De Marsily, G. and Tremosa, J. (2012). "Importance of thermo-osmosis for
500 fluid flow and transport in clay formations hosting a nuclear waste repository." *Earth and*
501 *Planetary Science Letters*, 339-340, 1-10.

502 Hong, P. Y., Pereira, J. M., Tang, A. M. and Cui, Y. J. (2013). "On some advanced thermo-
503 mechanical models for saturated clays." *International Journal of Numerical and Analytical*
504 *Methods in Geomechanics*, 37 (17), 2952-2971.

505 Hueckel, T. and Baldi, G. (1990). "Thermoplasticity of Saturated Clays: Experimental
506 Constitutive Study." *Journal of Geotechnical Engineering*, 10.1061/(ASCE)0733-
507 9410(1990)116:12(1778), 1778-1796.

508 Hueckel, T., François, B. and Laloui, L. (2011). "Temperature-dependent internal friction of
509 clay in a cylindrical heat source problem." *Géotechnique*, 61 (10), 831-844.

510 Laloui, L. and François, B. (2009). "ACMEG-T: Soil Thermoplasticity Model." *Journal of*
511 *Engineering Mechanics,* 10.1061/(ASCE)EM.1943-7889.0000011, 932-944.

512 Mitchell, J. K. (1993). *Fundamentals of Soil Behavior*, Wiley, University of California,
513 Berkley.

514 Moritz, L. and Gabrielsson, A. (2001). "Temperature Effect on the Properties of Clay." *Soft*
515 *Ground Technology*, 304-314.

516 Roshan, H. and Aghighi, M. A. (2012). "Analysis of Pore Pressure Distribution in Shale
517 Formations under Hydraulic, Chemical, Thermal and Electrical Interactions." *Transport in*
518 *Porous Media*, 92 (1), 61-81.

519 Roshan, H., Andersen, M. S. and Acworth, R. I. (2015). "Effect of solid-fluid thermal
520 expansion on thermo-osmotic test: An experimental and analytical study." *Journal of*
521 *Petroleum Science and Engineering*, 126, 222-230.

522 Sánchez, M., Gens, A. and Olivella, S. (2010). "Effect of thermo-coupled processes on the
523 behaviour of a clay barrier submitted to heating and hydration." *Annals of the Brazilian*
524 *Academy of Sciences*, 82(1), 153-168.

525 Sedighi, M. (2011). *An investigation of hydro-geochemical processes in coupled thermal,*
526 *hydraulic, chemical and mechanical behaviour of unsaturated soils*. Ph.D. Thesis, Cardiff
527 University, UK.

528 Sedighi, M., and Thomas, H. R. (2014). "Micro porosity evolution in compacted swelling
529 clays-A chemical approach." *Applied Clay Science*, 101, 608-618.

530 Sedighi, M., Thomas, H. R. and Vardon, P. J. (2016). "Reactive transport of chemicals in
531 unsaturated soils: Numerical model development and verification." *Canadian Geotechnical*
532 *Journal*, 52, 1-11.

533 Seetharam, S., Thomas, H. R. and Vardon, P. J. (2011). "Nonisothermal Multicomponent
534 Reactive Transport Model for Unsaturated Soil." *International Journal of Geomechanics,*
535 10.1061/(ASCE)GM.1943-5622.0000018, 84-89.

536 Soler, J. M. (2001). "The effect of coupled transport phenomena in the Opalinus Clay and
537 implications for radionuclide transport." *Journal of Contaminant Hydrology*, 53 (1-2), 63-84.

538 Sultan, N., Delage, P. and Cui, Y. J. (2002). "Temperature effects on the volume change
539 behaviour of Boom clay." *Engineering Geology*, 64, 135-145.

Thomas, H. R., He, Y., Sansom, M. R. and Li, C. L. W. (1996). "On the development of a model of the thermo-mechanical-hydraulic behaviour of unsaturated soils." *Engineering Geology*, 41, 197-218.

Thomas, H. R. and He, Y. (1997). "A coupled heat–moisture transfer theory for deformable unsaturated soil and its algorithmic implementation." *International Journal for Numerical Methods in Engineering*, 40 (18), 3421-3441.

Thomas, H. R., Cleall, P. J., Chandler, N., Dixon, D., and Mitchell, H. P. (2003). "Water infiltration into a large-scale in-situ experiment in an underground research laboratory." *Géotechnique*, 53 (2), 207-224.

Thomas, H. R. and Sedighi, M. (2012). "Modelling the engineering behaviour of highly swelling clays." *The 4th International Conference on Problematic Soils*, 21-23 September 2012, Wuhan, China, 21-33.

Thomas, H. R., Sedighi, M. and Vardon, P. J. (2012). "Diffusive reactive transport of multicomponent chemicals under coupled thermal, hydraulic, chemical and mechanical conditions." *Geotechnical and Geological Engineering*, 30 (4), 841-857.

Towhata, I., Kuntiwattanaku, P., Seko, I. and Ohishi, K. (1993). "Volume change of clays induced by heating as observed in consolidation tests." *Soils and Foundations*, 33 (4), 170-183.

Trémosa, J., Gonçalvès, J., Matray, J. M. and Violette, S. (2010). "Estimating thermo-osmotic coefficients in clay-rocks: II. In situ experimental approach." *Journal of Colloid and Interface Science*, 342, 175-184.

561 Vardon, P. J., Cleall, P. J., Thomas, H. R., Philp, R. N. and Banicescu, I. (2011). "Three-
562 Dimensional Field-Scale Coupled Thermo-Hydro-Mechanical Modeling: Parallel Computing
563 Implementation." *International Journal of Geomechanics,* 10.1061/(ASCE)GM.1943-
564 5622.0000019, 90-98.

565 Yang, Y., Guerlebeck, K. and Schanz, T. (2014). "Thermo-osmosis effect in saturated porous
566 medium." *Transport in Porous Media*, 104, 253–271.

567 Zheng, L. and Samper, J. (2008). "A coupled THMC model of FEBEX mock-up test."
568 *Physics and Chemistry of the Earth*, Parts A/B/C, 33, Supplement 1, S486-S498.

569 Zheng, L., Samper, J. and Montenegro, L. (2011). "A coupled THC model of the FEBEX in
570 situ test with bentonite swelling and chemical and thermal osmosis." *Journal of Contaminant*
571 *Hydrology*, 126, 45-60.

572 Zhou, Y., Rajapakse, R. K. N. D. and Graham, J. (1998). "A coupled thermoporoelastic
573 model with thermo-osmosis and thermal-filtration." *International Journal of Solids and*
574 *Structures*, 35, 4659-4683.

575

List of Tables:

List of Figures:

592 Table 1. Material parameters for verification exercise

Material parameters	**Value**
Porosity	0.4
Water density	998.0 $kg.m^{-3}$
Hydraulic conductivity	1.0×10^{-11} $m.s^{-1}$
Thermo-osmotic conductivity	5.0×10^{-12} $m^2.K^{-1}.s^{-1}$

593

594

595 Table 2. Material parameters for validation exercise

Material Parameters	**Value**	**Reference**
Porosity	0.4	François et al. (2009)
Solid density	2670.0 $kg.m^{-3}$	François et al. (2009)
Specific heat capacity of liquid	4186.0 $J.kg^{-1}.K^{-1}$	François et al. (2009)
Specific heat capacity of solid	732.0 $J.kg^{-1}.K^{-1}$	François et al. (2009)
Thermo-osmotic conductivity	$3.0x10^{-12}$ $m^2.K^{-1}.s^{-1}$	Gonçalvès et al. (2012)
Thermal conductivity	1.69 $W.m^{-1}.K^{-1}$	François et al. (2009)
Hydraulic conductivity	$1.5x10^{-12}$ $m.s^{-1}$	François et al. (2009)
Solid thermal expansion coefficient	$1.0x10^{-5}$ K^{-1}	François et al. (2009)
Water thermal expansion coefficient	$3.5x10^{-4}$ K^{-1}	François et al. (2009)
Water compressibility	$4.5x10^{-10}$ Pa^{-1}	François et al. (2009)
Soil compressibility	$4x10^{-9}$ Pa^{-1}	François et al. (2009)
Soil thermal expansion coefficient	$-5.0x10^{-5}$ K^{-1}	Hong et al. (2013)

596

597

598 Table 3. Material parameters for thermo-osmosis simulation

Material parameters	**Value**
Porosity	0.47
Solid density	2630.0 $kg.m^{-3}$
Specific heat capacity of liquid	4186.0 $J.kg^{-1}.K^{-1}$
Specific heat capacity of solid	937.0 $J.kg^{-1}.K^{-1}$
Thermo-osmotic conductivity	(1) 3.4×10^{-11} $m^2.K^{-1}.s^{-1}$ (2) 3.4×10^{-12} $m^2.K^{-1}.s^{-1}$ (3) 3.4×10^{-13} $m^2.K^{-1}.s^{-1}$
Thermal conductivity	1.55 $W.m^{-1}.K^{-1}$
Hydraulic conductivity	3.4×10^{-10} $m.s^{-1}$
Solid thermal expansion coefficient	3.0×10^{-5} K^{-1}
Water thermal expansion coefficient	3.5×10^{-4} K^{-1}
Water compressibility	4.5×10^{-10} Pa^{-1}
Soil compressibility	3.3×10^{-8} Pa^{-1}
Soil thermal expansion coefficient	-5.0×10^{-5} K^{-1}

599

600

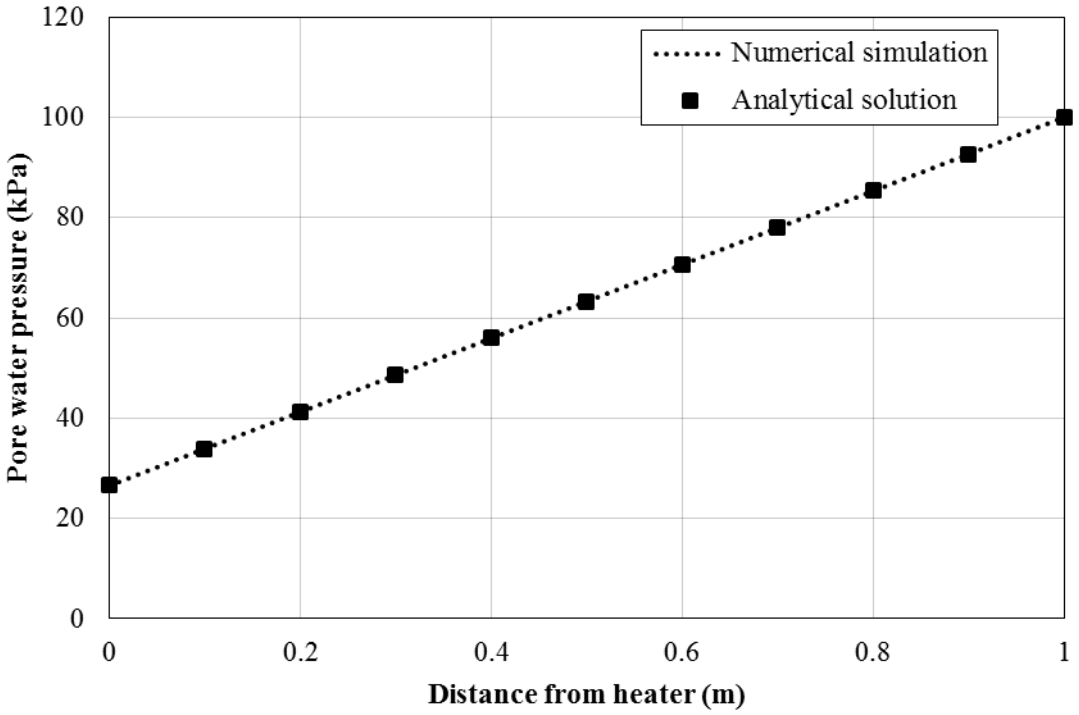

601

602 Fig. 1. Profile of pore water pressure in the domain at steady-state

603

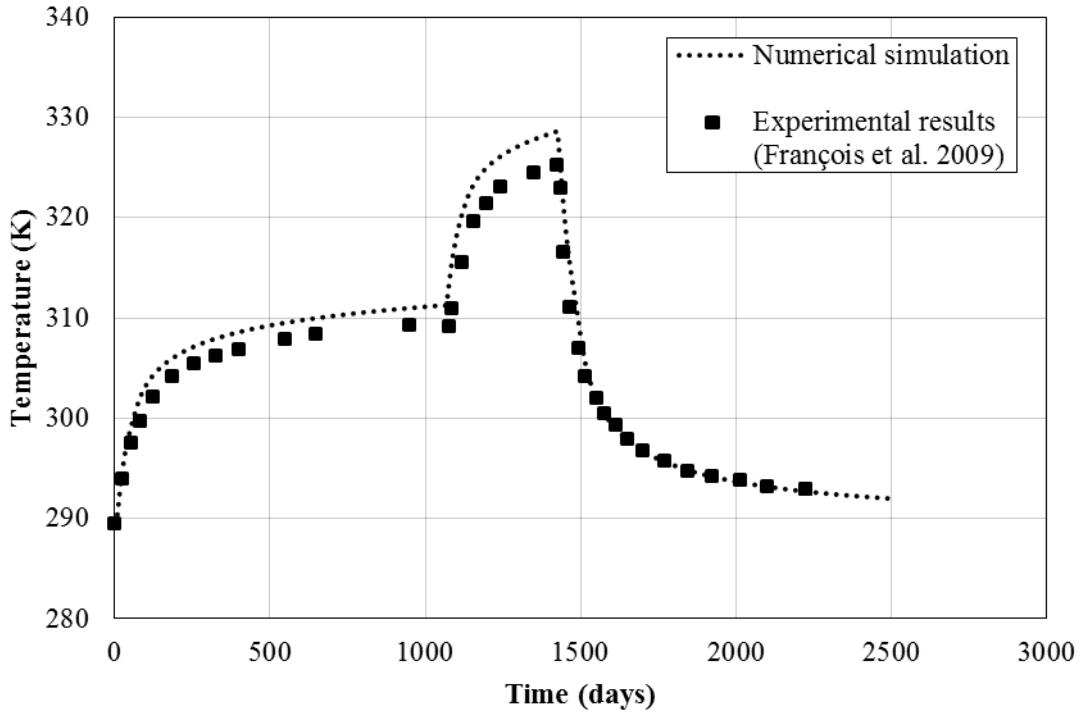

604

605 Fig. 2. Variation of temperature with time at the distance of 1.183 m from the axis of

606 symmetry

607

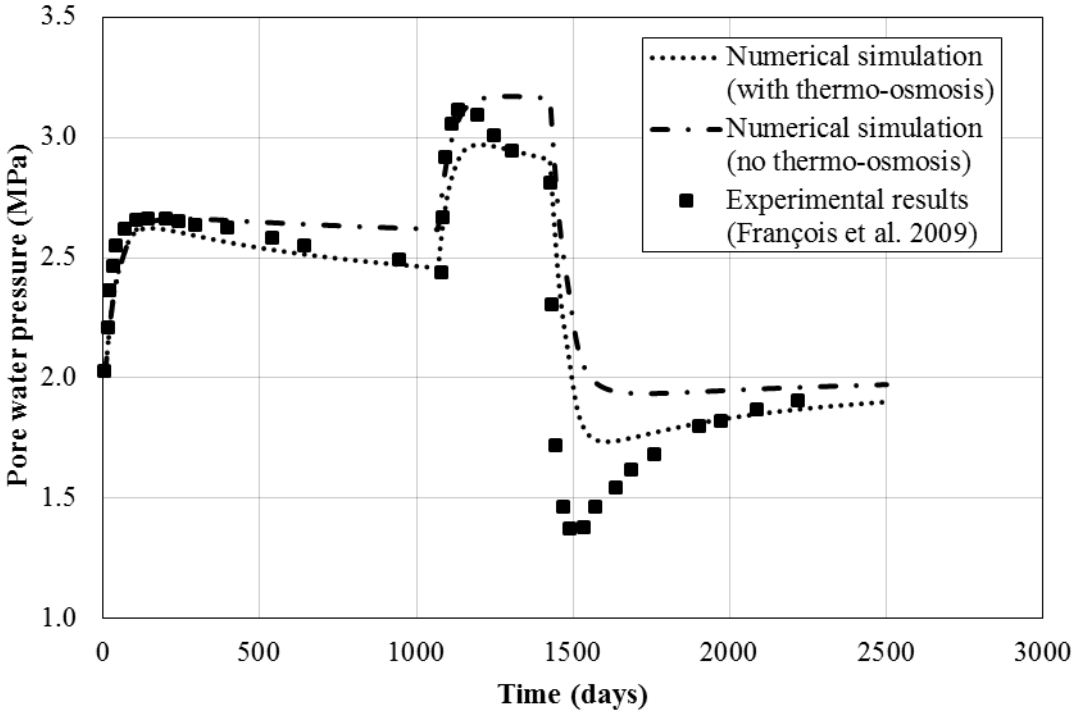

608

609 Fig. 3. Variation of pore water pressure with time at the distance of 1.183 m from the axis of

610 symmetry

611

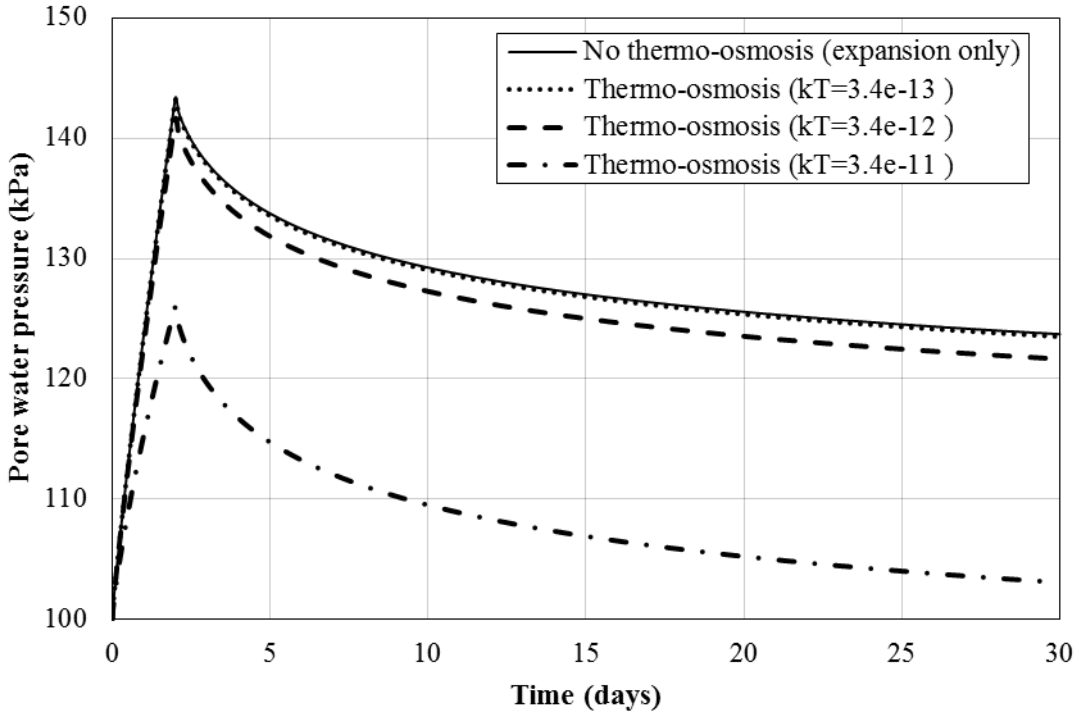

612

613 Fig. 4. Pore water pressure evolution with time at the heat source-soil interface

614

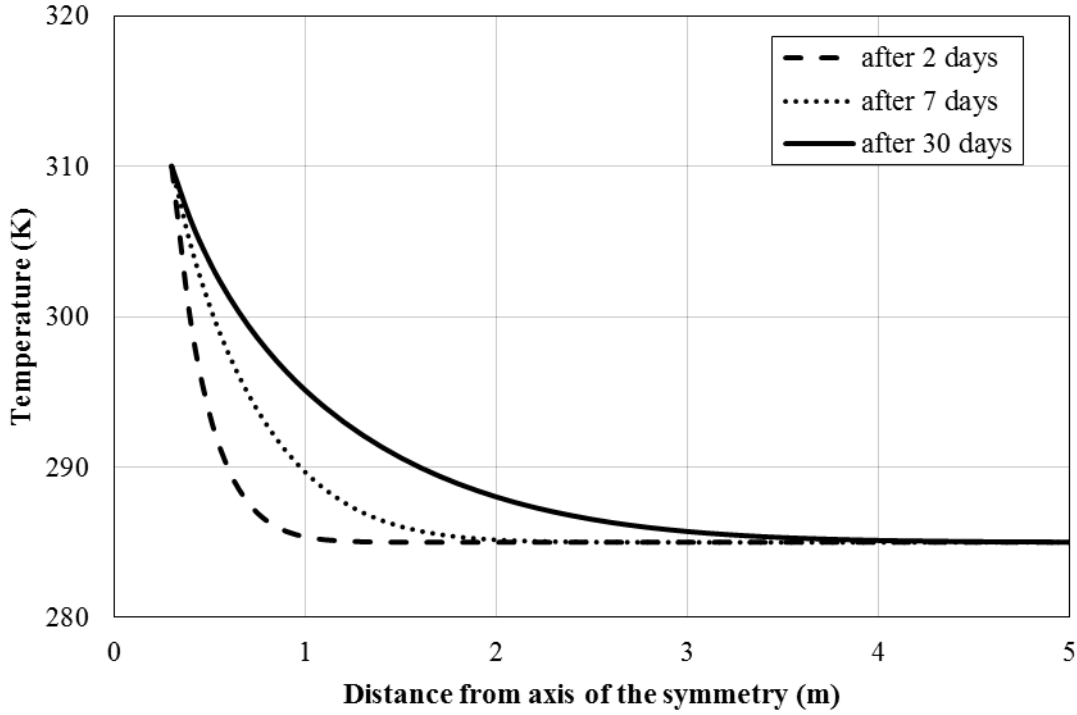

615

616 Fig. 5. Temperature distributions around the heat source after 2, 7 and 30 days of heating

617

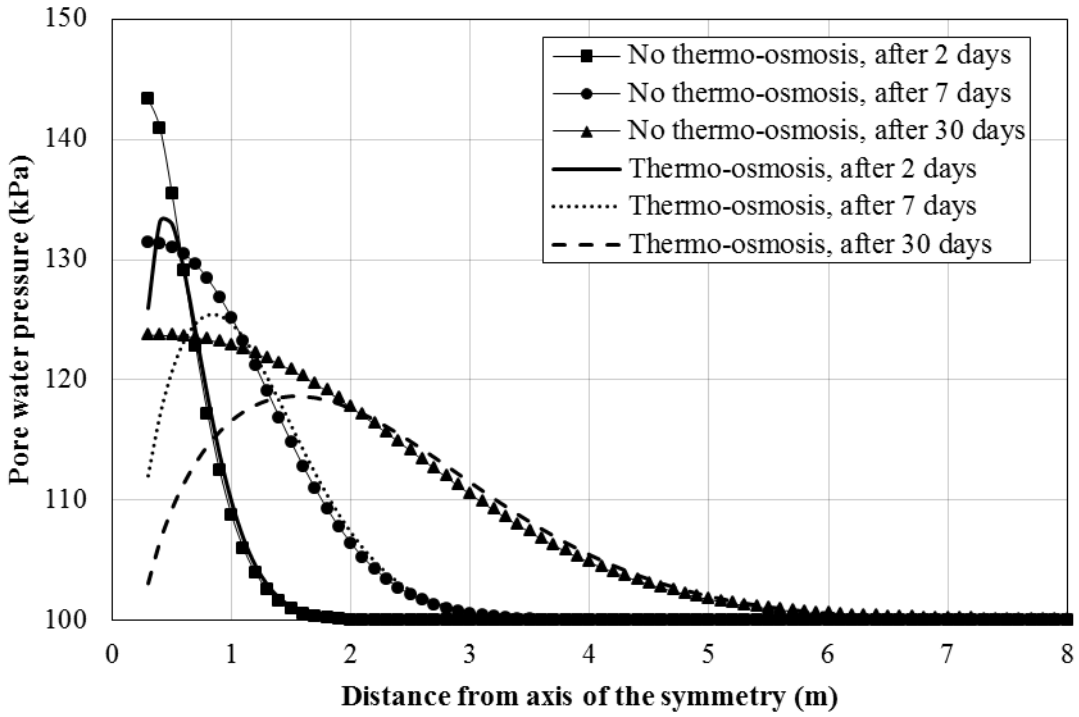

618

619 Fig. 6. Pore water pressure variation in the domain for the case of analysis without and with

620 thermo-osmosis ($k_T = 3.4\times10^{-11}$ $m^2.K^{-1}.s^{-1}$)

621